New Journal of Physics
An Institute of Physics and Deutsche Physikalische Gesellschaft Journal

PKE–Nefedov*: plasma crystal experiments on the International Space Station

Anatoli P Nefedov[1], Gregor E Morfill[2,9], Vladimir E Fortov[1], Hubertus M Thomas[2], Hermann Rothermel[2], Tanja Hagl[2], Alexei V Ivlev[2], Milenko Zuzic[2], Boris A Klumov[2], Andrey M Lipaev[1], Vladimir I Molotkov[1], Oleg F Petrov[1], Yuri P Gidzenko[3,5], Sergey K Krikalev[4,5], William Shepherd[5,8], Alexandr I Ivanov[4], Maria Roth[6], Horst Binnenbruck[6], John A Goree[7] and Yuri P Semenov[4]

[1] Institute for High Energy Densities, Russian Academy of Sciences, 127412 Moscow, Russia
[2] Centre for Interdisciplinary Plasma Science, Max-Planck-Institut für Extraterrestrische Physik, D-85740 Garching, Germany
[3] Y Gagarin Cosmonauts Training Centre, 141160 Star City, Moscow Region, Russia
[4] SP Korolev RSC Energia, Korolev 141070, Moscow Region, Russia
[5] Expedition 1 Crew, International Space Station (ISS)
[6] Deutsches Zentrum für Luft- und Raumfahrt (DLR), D-53227 Bonn, Germany
[7] Department of Physics and Astronomy, University of Iowa, Iowa City, IA 52242, USA
[8] National Aeronautics and Space Administration (NASA)
E-mail: gem@mpe.mpg.de

New Journal of Physics **5** (2003) 33.1–33.10 (http://www.njp.org/)
Received 28 November 2002, in final form 24 February 2003
Published 17 April 2003

Abstract. The plasma crystal experiment PKE–Nefedov, the first basic science experiment on the International Space Station (ISS), was installed in February 2001 by the first permanent crew. It is designed for long-term investigations of complex plasmas under microgravity conditions. 'Complex plasmas' contain ions, electrons, neutrals and small solid particles—normally in the micrometre range. These microparticles obtain thousands of elementary charges and interact with each other via a 'screened' Coulomb potential. Complex plasmas are of special interest, because they can form liquid and crystalline states (Thomas *et al* 1994 *Phys. Rev. Lett.* **73** 652–5, Chu and I 1994 *Phys. Rev. Lett.* **72**

* Named after Professor Anatoli Nefedov, who died on 19 February 2001.
[9] Author to whom any correspondence should be addressed.

PII: S1367-2630(03)56875-6

4009–12) and are observable at the kinetic level. In experiments on Earth the microparticles are usually suspended against gravity in strong electric fields. This creates asymmetries, stresses and pseudo-equilibrium states with sufficient free energy to readily become unstable. Under microgravity conditions the microparticles move into the bulk of the plasma (Morfill *et al* 1999 *Phys. Rev. Lett.* **83** 1598), experiencing much weaker volume forces than on Earth. This allows investigations of the thermodynamics of strongly coupled plasma states under substantially stress-free conditions. In this first paper we report our results on plasma crystals, in particular the first experimental observations of bcc lattice structures.

Microgravity studies of strongly coupled complex plasmas offer an exciting new field of research—investigations of the kinetics of self-organization (both in fluid flows and condensation/crystallization), research into the kinetic properties of surfaces (both steady and propagating structures), studies of the thermodynamics of homogeneous, inhomogeneous and stratified systems at the kinetic level etc. To enable such studies, the PKE–Nefedov laboratory—a Russian–German cooperation project—was launched and installed on the ISS. A detailed description of the laboratory, including the configuration of the plasma chamber, is given in the captions of figures 1 and 2.

The first set of experiments, the so-called 'basic experiments', performed at the beginning of March 2001 by the first permanent crew on the ISS, were designed to study the complex plasmas over a broad range of parameters. Monodisperse systems and binary mixtures were investigated at different argon pressures and rf powers. The neutral gas pressure was adjusted between 0.1 and 1.0 mbar in five steps where it was kept constant by a pressure control system. At each pressure, measurements were performed at five rf-power (forward) steps below 0.3 W. Typical trajectories of the microparticles are shown in overview in figure 3.

Under certain conditions we observed the formation of localized crystalline structures embedded in a fluid complex plasma state. In this experiment particles of 6.8 μm in diameter were dispersed into the plasma chamber. Plasma crystal structures can easily be identified in the lower central part of the plasma chamber. We identified the coexistence of domains of fcc, bcc and hcp structures (figure 4). For comparison with theory, the particle number density, n, was measured. It is found that the densities of the fcc and hcp lattice domains are almost equal ($n \approx 57.5$ and 57.8 mm^{-3}, respectively) and are smaller than the density of the bcc domains ($n \approx 67.0$ mm^{-3}).

In ground-based experiments, microparticles are always suspended in the sheath region above the lower rf electrode at a height z, where the volume forces—gravity and the sheath electrostatic force—balance each other, $QE_{\mathrm{sh}}(z) \approx Mg$. The z-dependence of the electric field leads to a strong gradient of the Coulomb coupling between neighbouring horizontal layers. The spatial scale of the coupling variation can be comparable to the mean interparticle distance, $\Delta = n^{-1/3}$: for 6.8 μm particles (even assuming pure Coulomb interaction) the ratio of the coupling force to the volume force, $Q^2/\Delta^2 Mg$, is about unity. Therefore, volume forces dominate and the lattice is highly stressed—the interparticle distance varies strongly in the vertical direction. In space experiments, on the other hand, the microparticles assemble themselves in the 'quasi-isotropic' bulk region of the discharge. Here, the weak (ambipolar) electric field is

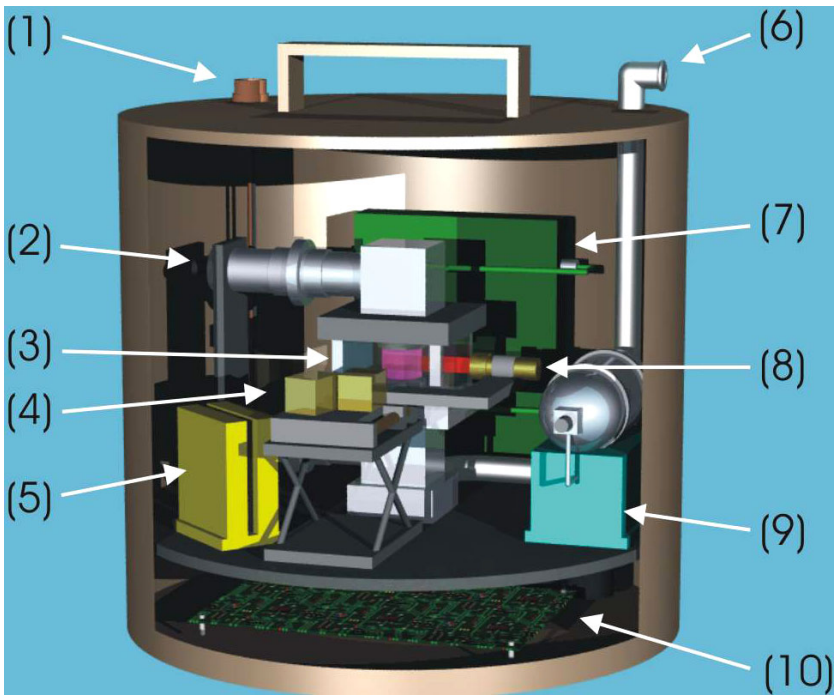

Figure 1. The PKE–Nefedov hardware onboard the ISS consists of two components—the experimental block and the so-called telescience module. The experimental block is shown in the figure. It can be divided into three different parts. Part I: the experimental set-up includes the rf plasma chamber (3); a sketch of the chamber is shown in figure 2 with assembled microparticle dispensers (2), rf generator (7), pressure control system (9), cameras (4) and lasers (8) mounted on a translation stage. The rf generator is a special development for very low rf power values, which are required for large and stable complex plasma systems and for plasma crystal formation. Two CCD cameras provide two different magnifications of the complex plasmas. The overview camera shows about a quarter of the field between the electrodes, 28.16×21.45 mm^2, while the high-resolution camera is used for detailed views inside the overview field covering 8.53×6.50 mm^2. On top of the experimental block a vacuum connection (6) is used to pump the experimental set-up. This vacuum port is contacted to outer space. Part II: electronics (5, 10) for part I and the system electronics (main power control). Part III: the experiment computer allows real time control of the plasma. Electrical signals produced by the experiment computer and the two video signals are contacted out of the container (1) and are controlled by the telescience module (not shown here). The computer visualizes the experimental data and can be used to control the experiment manually. Time codes (VITC signals) are inserted into the video frames and stored on two high-8 video recorders. The original video tapes are transferred to ground by the cosmonauts. The telescience module has the capability to transfer experimental data and video to ground and receive commands from ground, allowing full telescience control of the experiment by the scientists.

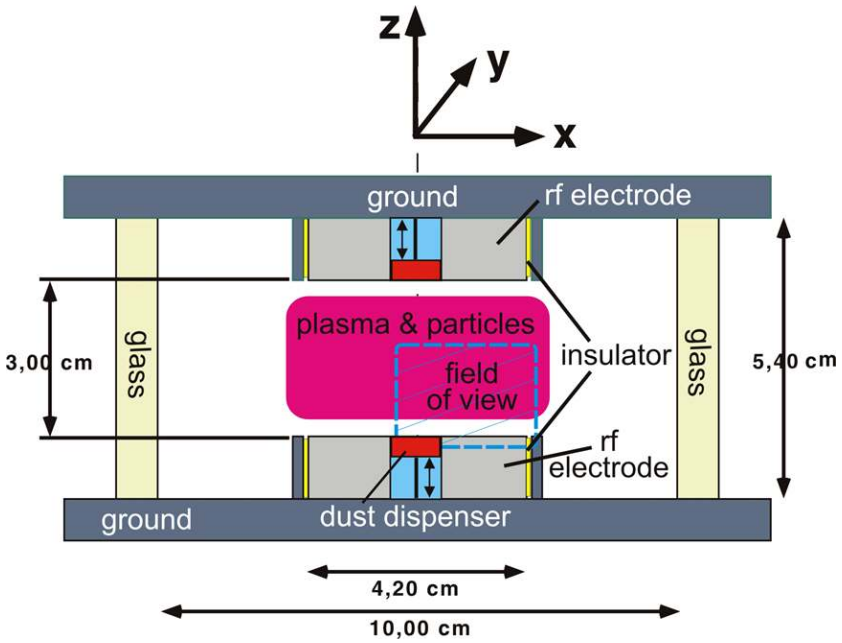

Figure 2. Sketch of the rf parallel plate discharge used in the PKE–Nefedov experiment. The plasma is excited between the two electrodes. The coupling of the rf to the electrodes is in push–pull mode. Monodisperse particles of different sizes—3.4 and 6.8 μm in diameter, as well as a mixture of both sizes—can be injected into the plasma chamber from two dispensers mounted in the upper and lower electrodes. The microparticles are illuminated by a thin ($\approx$150 μm) sheet of laser light perpendicular to the electrode system (produced by a laser diode and cylindrical optics). For each particle size one laser is installed, which is adjusted in power and optics to achieve best results. The reflected light from the microparticles is observed with two monochromatic video CCD cameras (768×576 pixels, 25 Hz, 8 bit) with different resolutions (the field of view for the overview camera is shown in the sketch). The microparticles can be identified in a single video frame and are then followed in time to investigate their dynamical behaviour. The frame rate is 25 Hz, which is faster than the complex plasma frequency of $\sim$10 Hz. Slow speed scanning of the laser and optics into the depth of the plasma chamber (y-direction) is used to measure the 3D positions of the microparticles.

$E_b \sim T_e/eL$, where $L \sim 3$ cm is the size of the discharge between the electrodes. Substituting values, this yields $E_b/E_{sh} \sim 10^{-2}$. This implies that in microgravity conditions the lattice (coupling) forces are about two orders of magnitude stronger than the volume forces, i.e., the system is weakly stressed. Hence plasma crystals produced in space are the most normal, isotropic, stress-free systems obtained so far.

In contrast to experiments on Earth [1, 2, 4]–[7], stringlike structures (when particles are aligned in vertical chains, the so-called 'hexagonal vertically aligned' lattice) have not been observed in microgravity conditions. Such structures are very prominent in plasma crystals with a few horizontal planes suspended in the sheath. The reason for the alignment is believed to be

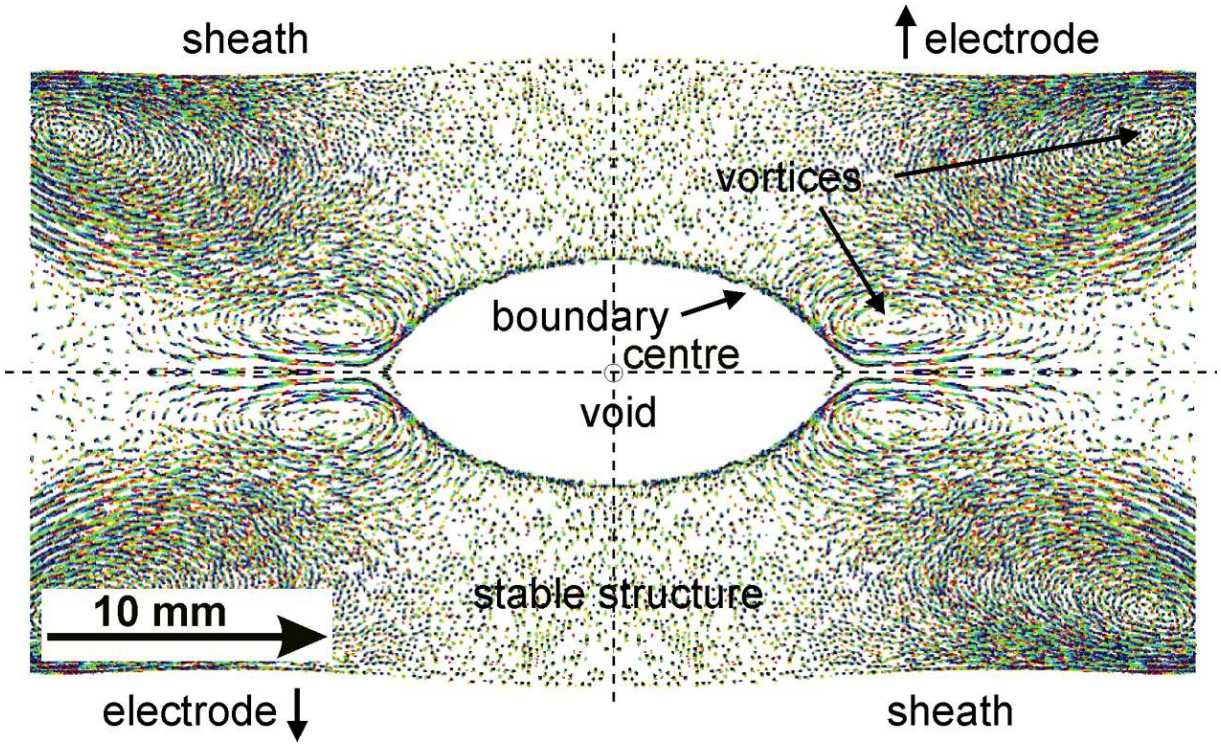

Figure 3. Colour coded trajectories of microparticles of 6.8 μm observed over 3 s. The observed original video image, covering approximately a quarter of the field shown here, was mirrored around the main chamber axes to show the full complex plasma structure and dynamics between the electrodes (not shown here). The main structural features are (1) the microparticle-free void in the centre, (2) the sharp boundary to the complex plasma, (3) the stable and regular structure along the vertical central axis and (4) the vortices along the horizontal axis and the outer edges.

the ion focusing downstream of the particle (ions are accelerated towards the electrode in the strong sheath field). This produces a wake (region of excessive positive charge) [8], and the lower particle can be trapped in the wake of the upper one. The weak ambipolar field in the bulk region cannot induce wake formation. Therefore, in microgravity experiments the interaction between particles is almost isotropic.

Thus, our observations are the first that can be compared directly with numerical simulations of strongly coupled Yukawa systems (where particles interact via a screened Coulomb, or Yukawa potential, $\propto e^{-r/\lambda}/r$) [9]. The phase diagram of the system can be conveniently defined for two variables: the coupling parameter, $\Gamma = Q^2/\Delta T$ (with T the particle temperature), and the lattice parameter, $\kappa = \Delta/\lambda$. To obtain a crystalline state, Γ must then be very large, because the fluid–solid phase transition is determined by the approximate condition $\Gamma(1+\kappa+\frac{1}{2}\kappa^2)e^{-\kappa} \geq 106$ [10]. Molecular dynamics calculations predict a transition from a bcc to an fcc crystalline state as the particle number density decreases (lattice parameter κ increases). The investigation of these theoretical predictions was the major aim of the work reported here.

Coexistence of bcc and fcc domains clearly indicates that our system is close to the corresponding phase equilibrium curve in the (Γ, κ) diagram. This implies that the lattice

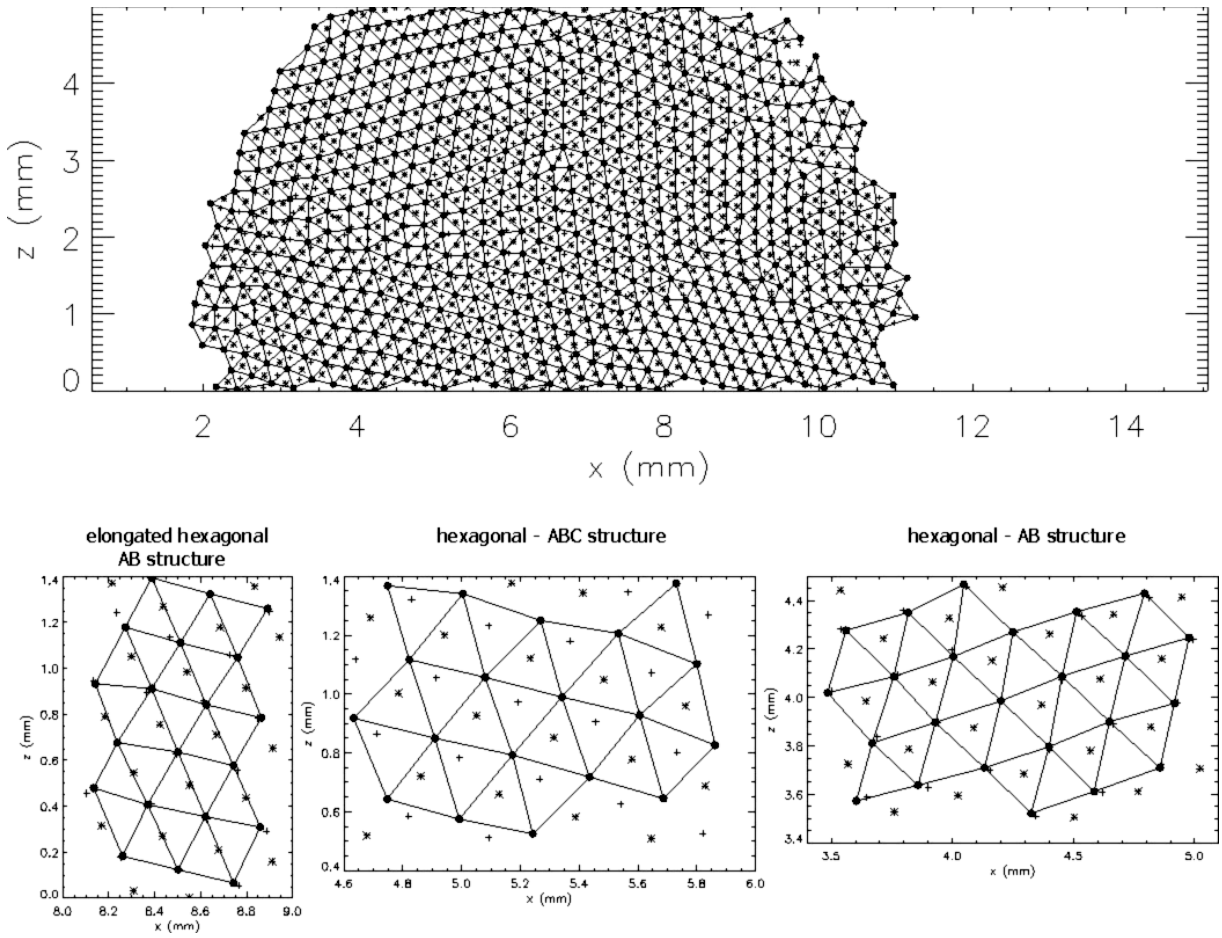

Figure 4. The symbols denote particle positions in the lowest three lattice planes. In addition a triangulation of the lower particle coordinates is plotted. In this experiment the plasma crystal was nearly flat at the lower boundary and in the centre. Different kinds of crystal domain can be distinguished, as presented in the lower part of the figure. In the left-hand plot an elongated hexagonal structure is shown (bcc-110 lattice type), the middle panel presents an alternating 'ABC' structure (fcc-111 lattice type) and the right-hand one represents an alternating 'AB' structure, which is known as an hcp structure. In some regions intermediate stages are also observed.

parameter κ must be about unity or higher [9]—i.e., that the electrostatic coupling is strongly screened. Further implicit evidence of the strong screening is the fact that the measured densities in the fcc and hcp domains are nearly equal: For $\kappa \geq 1$ the major contribution to the lattice energy is due to the coupling with the nearest neighbours, whose structures are *identical* for fcc and hcp lattices. In an fcc (hcp) lattice, there are $N_{\rm nn} = 12$ nearest neighbours, located at a distance $\Delta_{\rm nn} \approx 1.12\Delta$. The mean interparticle distance for the domain shown in figure 4 is $\Delta \approx 258\ \mu$m. For a bcc lattice, $N_{\rm nn} = 8$ and $\Delta_{\rm nn} \approx 1.09\Delta$, with $\Delta \approx 246\ \mu$m from figure 4. The coupling energy per particle is approximately $E \approx N_{\rm nn}(Q^2/\Delta_{\rm nn})\exp(-\Delta_{\rm nn}/\lambda)$. The phase equilibrium requires the pressure to be the same for all three domains: $p_{\rm cr} \sim n^2(\partial E/\partial n) = $ constant (for a crystal, the pressure $p_{\rm cr}$ is determined mostly by the coupling energy). Substituting the

measured densities of the bcc and fcc (hcp) domains we obtain an estimation for the screening length, $\lambda \approx 90\ \mu$m. Thus, we can conclude that for a typical plasma crystal the screening is strong—the lattice parameters are $\kappa_{\rm bcc} \approx 2.8$ for the bcc domains and $\kappa_{\rm fcc} \approx 3.0$ for the fcc (hcp) domains shown in figure 4.

Transition between fcc and hcp phases has never been considered in simulations, because both the coupling energy, $E(\kappa)$, and the harmonic entropy constant, $\Sigma(\kappa)$, of the fcc lattice are smaller than those of the hcp lattice for any κ [11]. Thus the Helmholtz free energy (per particle, normalized to T), $f = \Gamma E + \Sigma$, is smaller for an fcc lattice, and hence this is the thermodynamically preferred state. However, for $\kappa \geq 1$ the free energies of fcc and hcp phases should converge rapidly as κ increases, because only the next (after the nearest neighbour) 'shells' of surrounding particles can slightly change the value of f. Quantitatively, the relative difference in the coupling energy between hcp and fcc lattices is of the order of a few 10^{-5} for OCP systems ($\kappa < 1$) [12]–[14], and scales as $\propto e^{-\kappa}$ at large κ. In this case, small local fluctuations of the particle density and temperature might result in the transition from the equilibrium fcc to a metastable hcp phase and the hcp/fcc volume fraction should increase with κ and tend to 1/1 for $\kappa \gg 1$ (bcc domains should vanish because the preferred state for them is $\kappa \leq 1$). These fluctuations can be induced, for instance, by external excitation caused by the vortex motion shown in figure 3: hcp domains were only observed at the periphery, close to the regions where the vortices exist. Another possible reason for the hcp domains to appear is the particle size dispersion. The particles used in the experiment have quite a narrow size distribution, with a dispersion $\sigma_{\rm a} \equiv \sqrt{\langle \delta a^2 \rangle}/a \approx 1\%$. The size dispersion also implies a charge dispersion (since $Q \propto a$), which leads to an enormous number of possible particle configurations (and thus lattice energy levels, some of them metastable) within a given lattice type. The relative magnitude of the energy level splitting is of the order of $\sim\sigma_{\rm a}^2 \sim 10^{-4}$–$10^{-5}$. This energy variation exceeds the energy difference between hcp and fcc lattices, and hence for some particle configurations an hcp lattice might even be preferred. This is countered, however, by the observed size sorting—which, once completed, will introduce a large scale gradient.

The energy relaxation in strongly coupled systems proceeds much more slowly than in weakly coupled states (when the energy of each particle decays independently due to neutral gas friction). Transition from one metastable crystalline state to another, lower energy level can take dozens of minutes. This is shown in figure 5, in an MD simulation of the experiment described here. The decay of kinetic energy is clearly much longer than that given from Epstein gas drag. Presumably, this is because most of the energy is stored in the mutual electrostatic coupling, and each local transition between 'neighbouring' energy levels releases only a small fraction. Dynamically, we observed that the crystallization starts near the electrode and then propagates (sometimes, in the form of a smooth front) inward. Often, one can see transitions between different lattice plane orientations within the same lattice. This clearly indicates that the boundary conditions can be important for the equilibrium.

Even when the system reaches 'overall' lattice equilibrium, it can be 'noisy'—caged particles oscillate with rather low frequencies. This can lead to another process of energy splitting—due to the size dispersion, because of the possible existence of a few 'shallow' metastable states of the same levels (separated by potential hills of the order of the particle thermal energy). Then the whole system can continuously jump from one state to the other, yet keeping the same type of lattice.

Naturally, the measurements from the first 'basic experiments' need to be extended and the system properties need to be determined with increased precision. This includes in particular

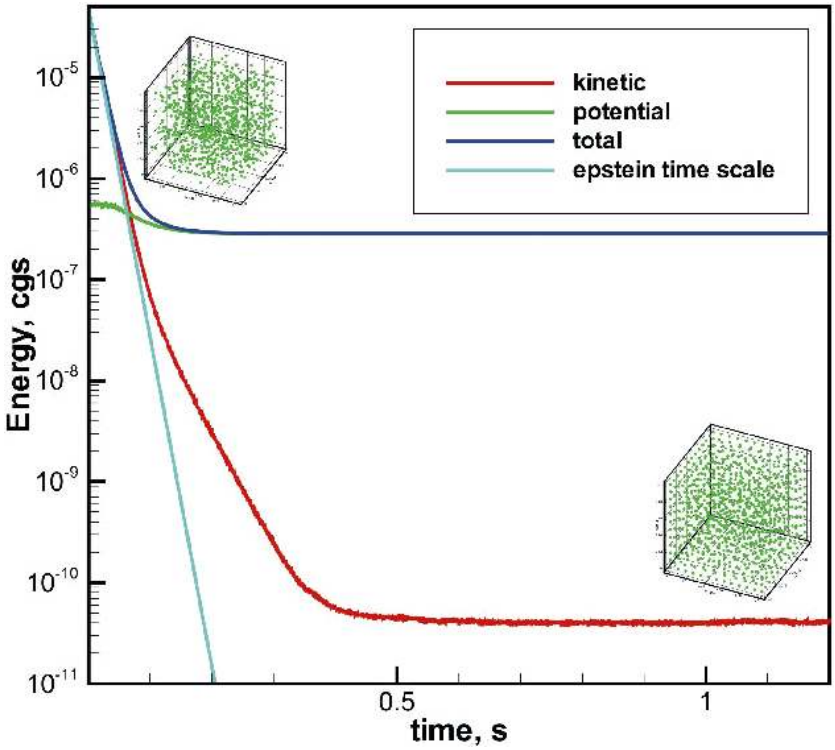

Figure 5. Temporal dependence of potential (green), kinetic (red) and total energy of microparticles embedded in neutral gas. The molecular dynamics method was used to describe the dynamics of the particles in a box with 'mirror' walls. Particles interact via a Yukawa potential. Parameters of the calculations correspond to a typical complex plasma experiment: particle number density 10^5 cm^{-3}, particle radius 3.5 μm, screening length 75 μm and neutral drag (Epstein) coefficient corresponds to a gas number density 10^{16} cm^{-3}. At $t = 0$ particles are randomly distributed in the box with random velocity distribution, and kinetic energy significantly larger than the potential energy. It is clearly seen that the initial decay of the total energy obeys the pure Epstein drag law. To calculate positions and velocities of the particles we use algorithm [13] for the proper finite difference scheme.

the time to reach equilibrium for different configurations and system sizes. At the same time, the demonstrated possibility to perform high-precision kinetic measurements of finite thermodynamic systems using complex plasmas under stress-free microgravity conditions should lead to increased efforts in numerical simulations and in the theoretical description of (e.g., microcanonical) small-system thermodynamics. The first observations with PKE–Nefedov certainly appear very promising for providing the experimental evidence on which to study some of these fundamental properties.

Summarizing, the first experiment conducted by PKE–Nefedov on the ISS was dedicated to the study of plasma crystals, formed spontaneously in a relatively stress-free environment under microgravity conditions. Co-existence of domains with different crystal structures (fcc, bcc and hcp) was observed—in particular the theoretically predicted bcc phase was seen for the first time. (Even the very large ground based systems investigated recently [15] did not find bcc structures.)

More detailed examination of the data allowed us, in addition, to investigate the correlation of crystal structural hierarchy with particle density. This is thermodynamically significant, since it directly concerns the energetics of equilibrium states under different (e.g., externally imposed) conditions. Our observations so far support the numerical simulation results regarding the transition from fcc to bcc lattices; however, the 'hcp anomaly' exists even in largely stress-free environments. This somewhat surprising observation requires further work. Experimentally the existence of hcp domains in plasma crystals could imply a source of self-excitation (or energy) in these systems not encountered before (some suggestions are made, e.g., external excitation, size dispersion), or it could be a long-term transient that is observed. MD simulations lend some support to the long-transient hypothesis. Alternatively, we have to remember that we are dealing with small (finite) systems, whose thermodynamic properties are not yet understood fully and for which a comprehensive theory has not yet been developed (see, however, [16]). Such systems are influenced strongly by the boundary conditions and energy input from the surroundings could be important. Again there is some experimental evidence that supports this. This is very interesting, since we could develop stress-free plasma crystals into a 'tool' to investigate small (microcanonical) thermodynamic systems under controlled conditions at the kinetic level for the first time, and observe some fundamental properties of such systems!

Acknowledgments

This work was supported by DLR/BMBF under grant no 50WM9852. The authors wish to acknowledge the excellent support from the PKE–Nefedov team (see below) and the agencies involved in making PKE–Nefedov a success: DLR, Rosavia-Cosmos, the Ministry of Industry, Science and Technologies, Russian Foundation for Basic Research, TSUP, RKK-Energia, Kayser-Threde, TSPK, IPSTC and the cosmonauts.

The PKE–Nefedov team (in alphabetical order) is M Belyaev, H Binnenbruck, V Blagov, L Deputatova, V Fortov, J Goree, S Goryainov, Y Grigoriev, W Griethe, T Hagl, A Ivanov, A Kellig, R Klett, C Körner, U Konopka, M Kudashkina, R Kuhl, S Kusnetsov, A Lebedev, A Lipaev, V Molotkov, G Morfill, A Nefedov, V Nikitsky, O Petrov, H Pfeuffer, M Pronin, I Roslavtzeva, T Rostopirov, M Roth, H Rothermel, P Saburov, G Schmidt, Y Semenov, A Sherbak, A Shurov, H Thomas and M Zuzic.

References

[1] Thomas H, Morfill G E, Demmel V, Goree J, Feuerbacher B and Möhlmann D 1994 *Phys. Rev. Lett.* **73** 652–5
[2] Chu J and I L 1994 *Phys. Rev. Lett.* **72** 4009–12
[3] Morfill G E, Thomas H M, Konopka U, Rothermel H, Zuzic M, Ivlev A and Goree J 1999 *Phys. Rev. Lett.* **83** 1598
[4] Hayashi Y and Tachibana K 1994 *Japan. J. Appl. Phys.* **33** L804–6
[5] Chu J H and I L 1994 *Physica* A **205** 183–90
[6] Pieper J B, Goree J and Quinn R A 1996 *Phys. Rev.* E **54** 5636–40
[7] Hayashi Y 1999 *Phys. Rev. Lett.* **83** 4764–7
[8] Schweigert V A *et al* 1996 *Phys. Rev.* E **54** 4155
[9] Hamaguchi S, Farouki R T and Dubin D H E 1997 *Phys. Rev.* E **56** 4671
[10] Vaulina O S and Khrapak S A 2000 *JETP* **90** 287–9
[11] Dubin D H E 2000 private communication
[12] Dubin D H E 1989 *Phys. Rev.* A **40** 1140–3

[13] Verlet L 1967 *Phys. Rev.* **159** 98–103
[14] Dubin D H E and O'Neil T M 1999 *Rev. Mod. Phys.* **71** 87–172
[15] Zuzic M, Goree J, Ivlev A V, Morfill G E, Thomas H M, Rothermel H, Konopka U, Sütterlin R and Goldbeck D D 2000 *Phys. Rev. Lett.* **85** 4064–7
[16] Gross D H E 2001 *World Scientific Lecture Notes in Physics* vol 66 (Singapore: World Scientific)